

# Study of a Method to Effectively Remove Char Byproduct Generated from Fast Pyrolysis of Lignocellulosic Biomass in a Bubbling Fluidized Bed Reactor

## **Authors:**

Jong Hyeon Ha, In-Gu Lee

*Date Submitted:* 2021-05-25

*Keywords:* biochar, bio-oil, inner and outer tubes, BFB reactor, fast pyrolysis, wood sawdust

## *Abstract:*

A critical issue in the design of bubbling fluidized bed reactors for biomass fast pyrolysis is to maintain the bed at a constant level to ensure stable operation. In this work, a bubbling fluidized bed reactor was investigated to deal with this issue. The reactor consists of inner and outer tubes and enables in situ control of the fluidized-bed level in the inner-tube reactor with a mechanical method during biomass fast pyrolysis. The significant fraction of biochar produced from the fast pyrolysis in the inner-tube reactor was automatically removed through the annulus between the inner and outer tubes. The effect of pyrolysis temperature (426–528 °C) and feeding rate (0.8–1.8 kg/h) on the yield and characteristics of bio-oil, biochar, and gaseous products were examined at a 15 L/min nitrogen carrier gas flow rate for wood sawdust with a 0.5–1.0 mm particle size range as a feed. The bio-oil reached a maximum yield of 62.4 wt% on a dry basis at 440 °C, and then slowly decreased with increasing temperature. At least 79 wt% of bio-char byproduct was removed through the annulus and was found in the reactor bottom collector. The GC-MS analysis found phenolics to be more than 40% of the bio-oil products.

*Record Type:* Published Article

*Submitted To:* LAPSE (Living Archive for Process Systems Engineering)

*Citation (overall record, always the latest version):*

LAPSE:2021.0408

*Citation (this specific file, latest version):*

LAPSE:2021.0408-1

*Citation (this specific file, this version):*


LAPSE:2021.0408-1v1

*DOI of Published Version:* <https://doi.org/10.3390/pr8111407>

*License:* Creative Commons Attribution 4.0 International (CC BY 4.0)

Article

# Study of a Method to Effectively Remove Char Byproduct Generated from Fast Pyrolysis of Lignocellulosic Biomass in a Bubbling Fluidized Bed Reactor

Jong Hyeon Ha <sup>1,2</sup> and In-Gu Lee <sup>1,\*</sup> 

<sup>1</sup> Energy Resources Upcycling Research Laboratory, Korea Institute of Energy Research, 152 Gajeong-ro Yuseong-gu, Daejeon 34129, Korea; gepde3@gmail.com

<sup>2</sup> Chemical and Biological Engineering Department, Korea University, 145 Anam-ro, Seongbuk-gu 02841, Korea

\* Correspondence: samwe04@kier.re.kr; Tel.: +82-42-8603559

Received: 16 October 2020; Accepted: 2 November 2020; Published: 4 November 2020



**Abstract:** A critical issue in the design of bubbling fluidized bed reactors for biomass fast pyrolysis is to maintain the bed at a constant level to ensure stable operation. In this work, a bubbling fluidized bed reactor was investigated to deal with this issue. The reactor consists of inner and outer tubes and enables in situ control of the fluidized-bed level in the inner-tube reactor with a mechanical method during biomass fast pyrolysis. The significant fraction of biochar produced from the fast pyrolysis in the inner-tube reactor was automatically removed through the annulus between the inner and outer tubes. The effect of pyrolysis temperature (426–528 °C) and feeding rate (0.8–1.8 kg/h) on the yield and characteristics of bio-oil, biochar, and gaseous products were examined at a 15 L/min nitrogen carrier gas flow rate for wood sawdust with a 0.5–1.0 mm particle size range as a feed. The bio-oil reached a maximum yield of 62.4 wt% on a dry basis at 440 °C, and then slowly decreased with increasing temperature. At least 79 wt% of bio-char byproduct was removed through the annulus and was found in the reactor bottom collector. The GC-MS analysis found phenolics to be more than 40% of the bio-oil products.

**Keywords:** wood sawdust; fast pyrolysis; BFB reactor; inner and outer tubes; bio-oil; biochar

## 1. Introduction

Since biomass is a carbon-based resource, it potentially produces all the types of fuels and chemicals which are presently obtained from crude oil. Furthermore, the use of biomass as a renewable energy carrier contributes to a reduction in the use of fossil fuels that are believed to be the major cause for global warming and environmental pollutions on the earth. Although many types of biomass resources are available for energy production, woody biomass is abundantly used to account for 87% of bioenergy produced in the world [1]. Currently, commercialized technologies that use woody biomass as an energy source are mostly direct burning methods including combustion in boiler systems [2], cofiring with coal in power plants [3], and burning in stoves [4]. A drawback of direct burning of woody biomass is the difficulty of long-term storage of the heat energy product. During recent decades, advanced thermochemical technologies have been developed for the conversion of lignocellulosic biomass to liquid or gas fuels [5]. Examples include fast pyrolysis [6], liquefaction [7], and gasification [8]. Fast pyrolysis and liquefaction both aim at the production of liquid biofuel, referred to as bio-oil, while gasification produces combustible syngas that can further undergo synthesis processes such as Fischer-Tropsch (FT) diesel to produce liquid hydrocarbon fuels [9] and dimethyl

ether (DME) [10]. In particular, biomass fast pyrolysis receives a great amount of attention because it is operated at atmospheric pressure to produce bio-oil with high yields (up to 75 wt%) [9], while biomass liquefaction generally requires high pressures of 4–22 MPa [7,11]. Since bio-oil is a liquid material, it can be stored and transported by using current infrastructures used for petroleum fuels.

Bio-oil from fast pyrolysis of woody biomass has a dark brown color and a water content of more than 15 wt%, depending on the moisture content of the woody biomass used and pyrolysis conditions. Bio-oil is known to contain hundreds of organic compounds such as acids, alcohols, ketones, aldehydes, phenols, ethers, esters, sugars, furans, alkenes, nitrogen compounds, and miscellaneous oxygenates [12]. Pyrolysis bio-oil has undesirable characteristics as a fuel such as low heating values of 14–18 MJ/kg (LHV) due to high contents of oxygen and low pH values caused mostly by the presence of carboxylic acids [13]. It also contains small amounts of solids such as ash and carbon residue, which generally have a negative effect on bio-oil as a fuel [14]. Nevertheless, considerable efforts have been given regarding the application of pyrolysis bio-oil to combustion systems including boilers, diesel engines, and gas turbines [15,16]. For more effective applications, upgrading of pyrolysis bio-oil has also been studied by physical methods such as emulsification with diesel or blending with alcohols [16] and thermochemical methods such as hydrothermal upgrading [17], hydroprocessing consisting of hydrodeoxygenation (HDO) and hydrocracking [18], or catalytic cracking [19]. A wide range of potential applications of pyrolysis bio-oil as a source of fuel or value-added chemicals has led to the development of a more efficient biomass fast pyrolysis process [20,21].

In comparison with conventional slow pyrolysis used usually for the production of charcoal [22], fast pyrolysis of woody biomass to maximize bio-oil production requires much higher heating rates of 10–200 °C/s along with a shorter reactor residence time of a few seconds at temperatures of approximately 500 °C [6,20,23]. A variety of reactor configurations have been developed to achieve high heating rates in biomass fast pyrolysis, including a bubbling fluidized bed reactor [24–27], circulating fluidized bed reactor [28,29], entrained flow reactor [30], vortex reactor [31], cyclone reactor [32], centrifuge reactor [33], free fall reactor [34], rotating cone reactor [35], and screw reactor [36]. Among those reactor configurations, the bubbling fluidized bed reactor has received much attention due to its advantages of relatively simple construction and operation, easy scale-up, and familiar technology [20].

A critical issue to be addressed in the design of a bubbling fluidized bed reactor for biomass fast pyrolysis is how to maintain the bed at a constant level by steadily removing biochar byproduct from the reactor. In the conventional process, biochar is removed from the bed together with gas and vapor products by a carrier gas, thereby maintaining the bed at a constant level [21]. The biochar exiting from the reactor consecutively enters a cyclone and is separated from the other products. To realize complete removal of the biochar (yields up to 20 wt%) from the bubbling bed by this method, it is important to prepare for woody biomass feed with very small particle sizes [21] because big wood particles proportionally produce a big-sized biochar byproduct which can accumulate in the bed and enhance the bubbling bed. The increasing bubbling bed results in variations in pressure drop and fluidization characteristics in the reactor, which have negative influences on the operation and productivity.

To the best of our knowledge, little work has focused on in situ removal of biochar byproducts from a bubbling fluidized bed reactor through mechanical methods in order to maintain the bubbling bed constant. In this work, a double-tube type of bubbling fluidized bed reactor was designed and tested for the fast pyrolysis of wood sawdust. This reactor aims at maintaining the bubbling bed at a constant level by a mechanical method, which allows a wider range of operating conditions during fast pyrolysis of woody biomass.

## 2. Materials and Methods

### 2.1. Materials

Pine sawdust obtained from a local sawmill was dried and sieved to have a particle size range of 0.5–1.0 mm, before the use in the fast pyrolysis experiments as a feed. Pine is one of the most abundant

wood species in Korea. Characteristics of the pine sawdust feed are listed in Table 1. The volatile matter of the feed was 73.7 wt%, which provided an expectation for the maximum yield of bio-oil formed by fast pyrolysis reaction. Sand obtained from a local area was used as a fluidizing medium. The sand was washed with deionized water several times followed by drying at 105 °C, in an oven and screening, to obtain particle sizes between 0.4–0.8 mm before use in the reactor. Nitrogen gas (purity >99.5%) was used as a carrier gas in the pyrolysis reaction.

**Table 1.** Characteristics of wood sawdust feed.

Proximate Analysis <sup>a</sup> (wt%)				Ultimate Analysis <sup>b</sup> (wt%)				Heating Value <sup>c</sup> (MJ/kg)		
M	VM	FC	Ash	C	H	N	S	O <sup>d</sup>	HHV	LHV
9.7	73.7	16.0	0.5	45.5	7.0	0.6	0.002	46.9	17.9	16.1

<sup>a</sup> M, moisture; VM, volatile matter; FC, fixed carbon. <sup>b</sup> Ultimate analysis was on a dry basis. <sup>c</sup> Heating value was on a dry basis. <sup>d</sup> Calculated by the difference, 100—(C + H + N + S).

## 2.2. Methods

A schematic diagram of the reaction system used for the fast pyrolysis of wood sawdust is illustrated in Figure 1. The reactor consisted of two tubes in annulus form (inner and outer tubes). The diameters of the inner and outer tubes were 50 and 75 mm, respectively, and the annulus between two tubes was about 10 mm. Fast pyrolysis of wood sawdust occurred in the bubble-fluidized bed of the inner tube. An amount of sand medium was placed on the distributor and preheated nitrogen gas was delivered through a combination of gas chamber and distributor to heat and fluidize the sand medium in the reactor. A measured amount of wood sawdust was put in the hopper and delivered into the inner tube reactor with a screw feeder to begin the fast pyrolysis reaction. Electrical furnaces were used to provide process heat to the nitrogen preheater, gas chamber, reactor, free board, and cyclone. In particular, a three split-zone furnace was installed outside the outer tube of the reactor to achieve an independent control of the reaction temperatures of T3, T4, and T5, as shown in Figure 1. The fast pyrolysis reaction resulted in the formation of vapor and char products which had different properties. The vapor product quickly flowed up in the inner tube to the free board along with the carrier gas and was separated from the sand medium. The char product underwent the same procedure as the vapor product but its residence time in the reactor was expected to be much longer than the vapor product. Consequently, a significant amount of char product was expected to remain in the reactor and caused an increase in the fluidizing bed. Since the increase in the fluidizing bed could change reaction conditions such as temperature, pressure, and thereby product yields, it was very important to maintain the fluidized bed at a constant level. The reaction system, shown in Figure 1, was designed to control the maximum fluidizing bed level by the height of the inner reactor tube. The char product of big particle sizes which passed over the end of the inner tube reactor was dropped down through the annulus between the inner and the outer tubes and the char product of small particle sizes and coke formed continued to pass through the free board into the cyclone where it was separated from the vapor product. The char product which was dropped down through the annulus was accumulated in the bottom-char collector, and then regularly removed from the reactor during the pyrolysis reaction. The char product and coke collected in the cyclone were also removed by opening the valve below the cyclone. The vapor product that passed through the cyclone entered a shell and multi-tube type condenser in which the vapor was quickly quenched and divided into permanent gas and liquid product (bio-oil). A chiller (JEIO TECH, RW-3040G) at −10 °C was used to operate the condenser. The bio-oil product was collected in the bottom of the condenser and gaseous product underwent further purification steps (second and third bio-oil collectors) to separate any remaining fraction of bio-oil product. A gas sample was obtained at the gas sample outlet and collected in a 0.5 L gas tight bag for compositional analysis.

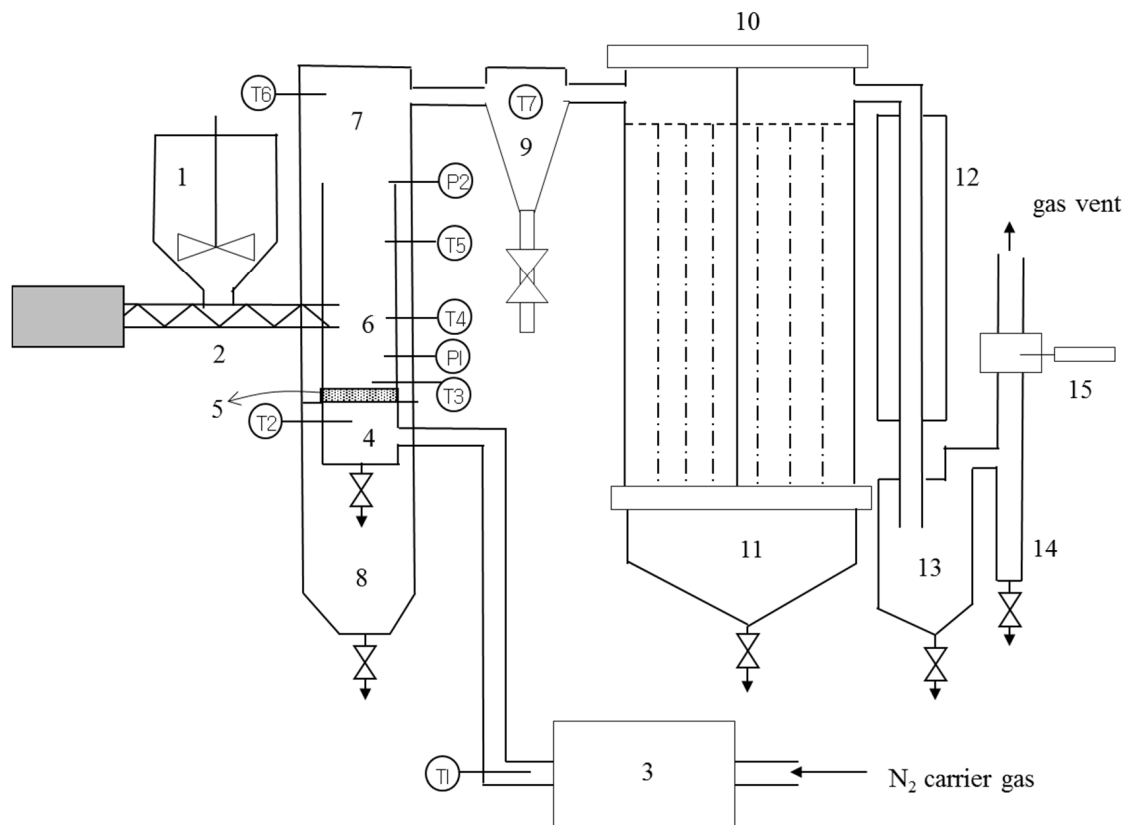


**Figure 1.** Schematic diagram of the biomass fast pyrolysis system. (1) Hopper; (2) Screw feeder; (3) Carrier gas preheater; (4) Gas chamber; (5) Distributor; (6) Pyrolysis reactor; (7) Free board; (8) Reactor bottom-char collector; (9) Cyclone; (10) Condenser; (11) First bio-oil collector; (12) Cooler; (13) Second bio-oil collector; (14) Third bio-oil collector; (15) Gas sample outlet.

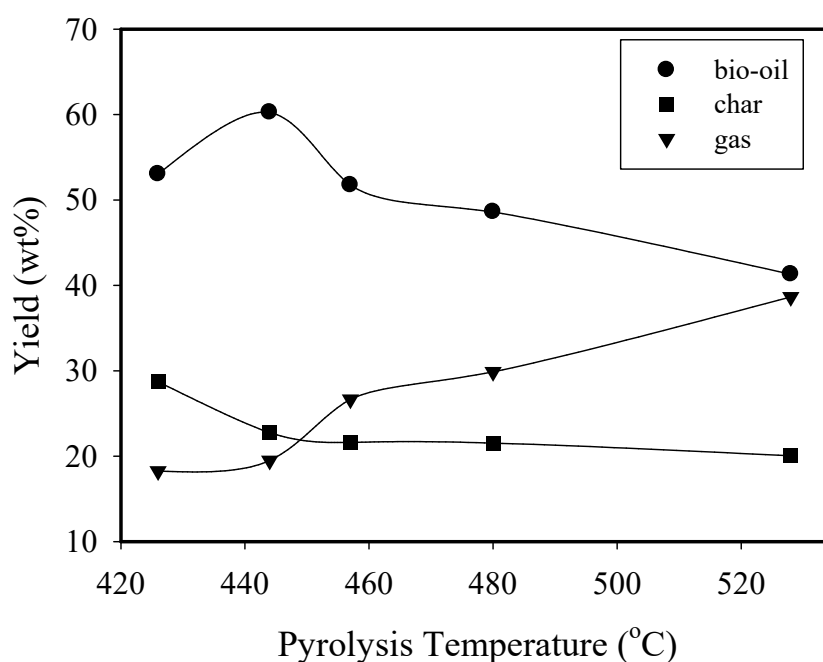
### 2.3. Analyses

Proximate and ultimate analyses of wood sawdust feed and pyrolysis products, such as bio-oil and biochar, were accomplished by independent organizations with a thermogravimeter (LECO Co., TGA-701) and an elemental analyzer (LECO Co., TruSpec), respectively. Sulfur content of the feed and biochar product was determined by a sulfur analyzer (LECO CO., SC-432DR) and heating value was analyzed with a calorimeter (LECO Co., AC600). Water content of bio-oil was measured by a Karl Fisher Titrator (METTLER TOLEDO, V20). Identification of organic compounds present in bio-oil product was accomplished by a GC-MSD system (GC, AGILENT 7890A and MSD, AGILENT 5977A) with helium (purity 99.999%) as the carrier gas. A HP-5MS column was used at 45 °C for 5 min followed by a ramp of 8 °C/min to 100 °C, a 3 min hold at 100 °C, an 8 °C/min ramp to 220 °C, and a 1 min hold at 220 °C. Compositional analysis of gaseous product was performed by a GC (DS SCIENCE, IGC 7200) equipped with a thermal conductivity detector for H<sub>2</sub>, CO, CO<sub>2</sub>, and CH<sub>4</sub> and a flame ionization detector for C<sub>2</sub>H<sub>4</sub>, C<sub>2</sub>H<sub>6</sub>, C<sub>3</sub>H<sub>6</sub>, and C<sub>3</sub>H<sub>8</sub> species. A mixture of 8 vol% hydrogen in helium was used as a carrier gas. A Carboxen-1000 packed column was operated at 35 °C for 4.2 min followed by a 15 °C/min ramp to 227 °C, 30 °C/min to 350 °C, and a 2 min hold at 350 °C. Chemical oxygen demand of bio-oil was measured by a closed reflux titrimetric method. Total organic carbon of bio-oil product was measured by an independent organization with a TOC analyzer (ELEMENTAR, vario TOC cube). Acidity of bio-oil product was determined by a pH meter (DKK-TOA, IM-30R).

### 3. Results and Discussion

#### 3.1. Distribution of Product

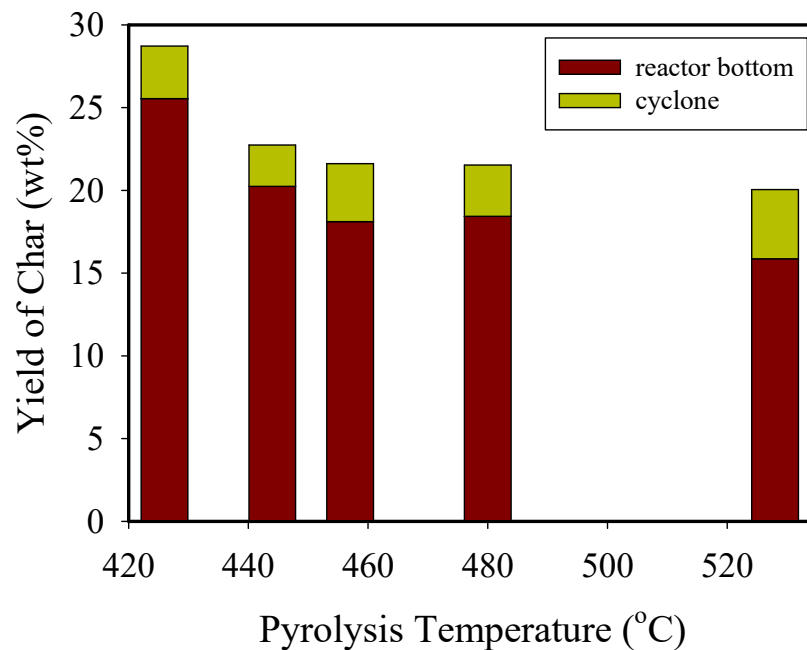
In the field of biomass fast pyrolysis, reaction temperature and heating rate are considered to be the most important parameters to determine product distribution [21]. Therefore, this work investigated the influence of pyrolysis temperature and sawdust feeding rate on the distribution and characteristics of products under the conditions of atmospheric pressure and a nitrogen carrier gas flow rate of 15 L/min. The increase in feeding rate at the same reaction temperature resulted in the increase in heating rate. Figure 2 shows the variations in the yield of bio-oil, biochar, and gas products with pyrolysis temperature. In this work, pyrolysis temperature was taken as the average of three temperatures, i.e., T3, T4, and T5, in the inner tube of the reactor shown in Figure 1. The yield of bio-oil showed a maximum value of 60.3 wt% at 444 °C, and then decreased steadily with increasing temperature. Meanwhile the yield of gaseous product increased continuously from 18.3 wt% at the lowest temperature of 426 °C to 38.7 wt% at the highest temperature of 528 °C examined. The yield of biochar product with pyrolysis temperature showed an opposite trend to gaseous product with a higher decrease at a lower temperature range between 426 and 457 °C. It can be said that most of the enhanced fraction of gaseous product with increasing temperature above 444 °C was attributed to the gasification of organic compounds in bio-oil vapor. This gasification reaction probably occurred in the downstream zone of the inner tube reactor and in the free board. In a related work using a circulating fluidized bed reactor, Xianwen et al. [28] found that a higher temperature contributed to secondary reactions such as gasification, resulting in a decrease in bio-oil yield. The biochar product was obtained from the two collection systems (reactor bottom and cyclone).



**Figure 2.** Effect of pyrolysis temperature on the product distribution for fast pyrolysis of wood sawdust (0.8 kg/h feeding rate, 15 L/min N<sub>2</sub> carrier gas flow rate).

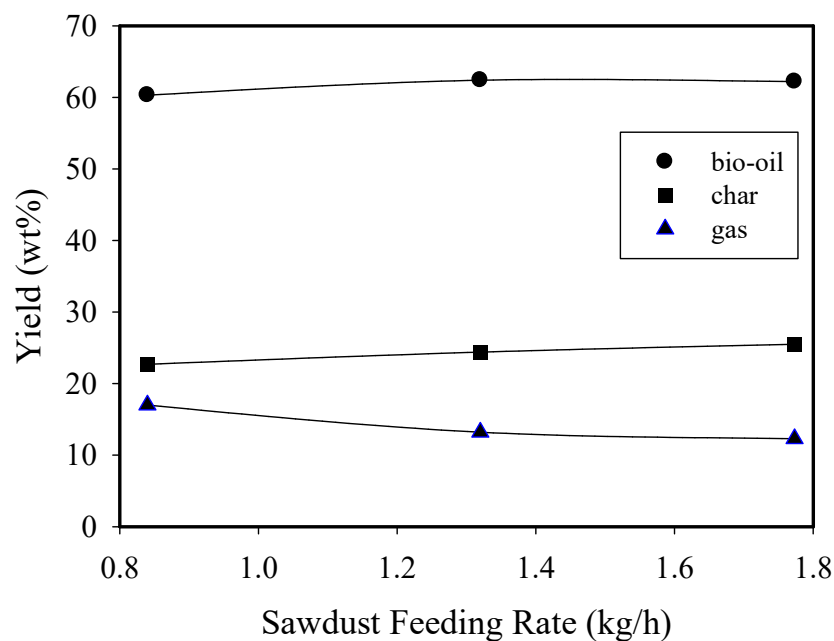
As shown in Figure 3, most of the total biochar was obtained from the reactor bottom collector over the temperature range examined. A higher pyrolysis temperature seems to give a slightly lower yield of biochar product from the reactor bottom collector with 89 wt% at 426 °C and 79 wt% at 528 °C. These data demonstrate the fact that the double-tube type of fluidized bed reactor, employed in this work, is able to greatly reduce the load of biochar in the cyclone present after the bubbling fluidized bed (BFB) reactor. Furthermore, this type of pyrolysis reactor can effectively control the fluidized bed

at a constant level by the height of the inner tube reactor. As a result, a stable operation can be achieved for a long period of time owing to a constant bubbling bed, which is conventionally controlled by removing all the char byproduct along with gases (carrier gas and product gas) and vapors [21].



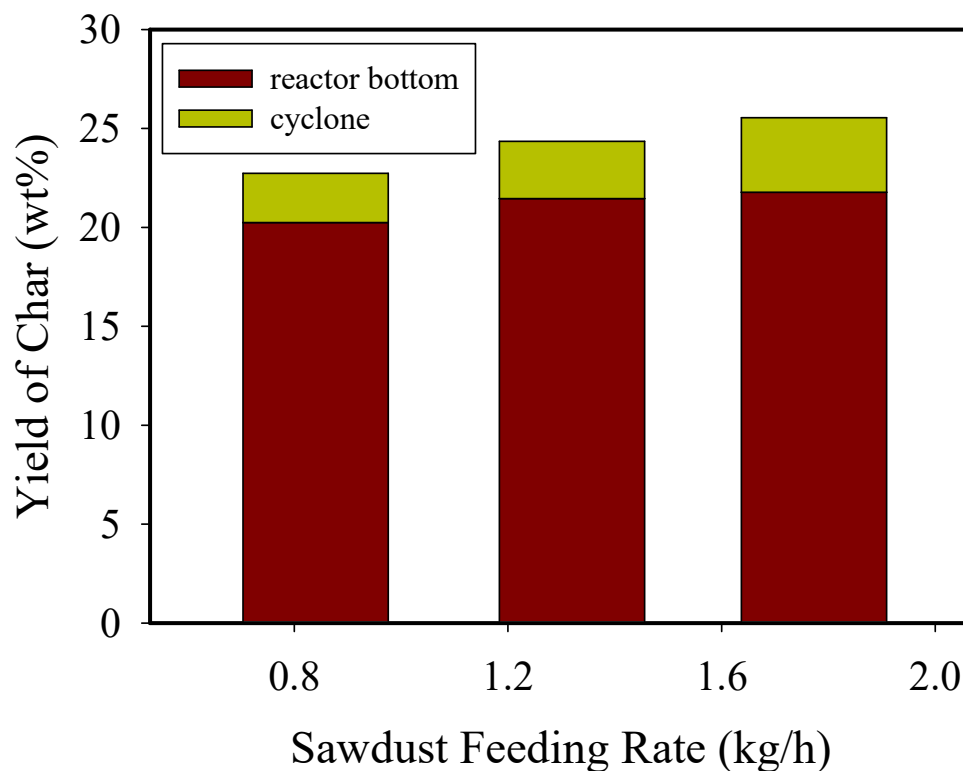
**Figure 3.** Distribution of char product at different pyrolysis temperature for fast pyrolysis of wood sawdust (0.8 kg/h feeding rate, 15L/min N<sub>2</sub> carrier gas flow rate).

Figure 4 shows variation in the yield of pyrolysis products with a pine sawdust feeding rate at 440 °C and 15 L/min carrier gas flow rate. A change in the feeding rate, in the range from 0.8 to 1.8 kg/h, had little influence on the product distribution with a slight increase in bio-oil and biochar products combined with a decrease in gaseous product. Park et al. [37] found similar results from the fast pyrolysis of pine sawdust in their bubbling-bed reactor.



**Figure 4.** Effect of sawdust feeding rate on the product distribution for fast pyrolysis of wood sawdust (440 °C pyrolysis temperature, 15 L/min N<sub>2</sub> carrier gas flow rate).

Figure 5 illustrates the variation in the distribution of biochar product with increasing sawdust feeding rate. As expected, a higher feeding rate resulted in greater yield of biochar from the cyclone, due to the increasing amount of vapor formed by the fast pyrolysis reaction. Nevertheless, biochar obtained from the cyclone, even at about 1.7 kg/h sawdust feeding rate, was less than 15 wt% of the amount of total biochar collected.



**Figure 5.** Distribution of char product at different sawdust feeding rate (0.8 kg/h feeding rate, 15 L/min N<sub>2</sub> carrier gas flow rate).

### 3.2. Characterization of Products

The characteristics of the mixtures of bio-oil products obtained from three different collection systems are displayed in Table 2. The ultimate analysis shows that the bio-oil products have lower carbon content along with higher oxygen and hydrogen contents than the sawdust feed in all the pyrolysis cases. As a result, the bio-oil product has slightly higher O/C and H/C ratios than the sawdust feed. It is known that most of the original oxygen present in biomass feedstocks remains in bio-oils after fast pyrolysis [13], in the form of oxygenated compounds and water [14]. The pyrolysis temperature did not significantly influence the elemental composition of the bio-oil products, while higher sawdust feeding rate increased carbon content and decreased oxygen content of the bio-oil products. It was suspected that carbon consisting of crystalline cellulose of the sawdust feed mostly remained in the biochar. Nitrogen in the feed was likely to remain in bio-oil rather than in biochar during pyrolysis reaction. The water content of the bio-oil products ranged between 30 and 50 wt%, which was much higher than the moisture content of the wood sawdust feed. At least 33 wt% of the water present in bio-oil was calculated to be formed during the fast pyrolysis reaction, depending the reaction conditions. Water may have been formed by dehydration reaction [13]. The heating value of the bio-oil products was slightly lower than the sawdust feed due to the higher water content. The low pH value of the bio-oil products was probably due to the high concentration of the organic acids present in the bio-oils.



**Table 2.** Effect of pyrolysis temperature and feeding rate on the fuel characteristics of bio-oil.

	Pyrolysis Temperature (°C) at 0.84 kg/h Feeding Rate					Sawdust Feeding Rate (kg/h) at 440 °C		
	426	444	457	480	528	0.84	1.32	1.77
Yield (wt%)	53.0	60.3	51.7	48.1	41.3	60.3	62.4	62.2
Elemental comp. (wt%)								
C	34.2	43.2	39.3	41.3	32.3	43.2	40.1	39.9
H	9.1	10.1	10.1	9.8	9.1	10.1	9.9	9.8
N	0.9	1.2	0.9	0.9	0.9	1.2	0.9	0.1
O <sup>a</sup>	55.8	45.5	49.7	48.0	57.7	45.5	49.1	50.2
O/C (mol/mol)	1.22	0.79	0.95	0.87	1.34	0.79	0.92	0.94
H/C (mol/mol)	3.19	2.81	3.08	2.85	3.38	2.81	2.96	2.95
Water content (wt%)	36.4	35.4	36.8	30.7	49.2	35.4	34.5	40.6
HHV (MJ/kg)	17.12	17.46	17.12	17.12	17.12	17.46	16.79	16.87
TOC (g/L)	384.6	383.6	366.5	410.6	310.5	383.6	404.9	364.1
COD (gO <sub>2</sub> /L)	1328	1216	1344	1288	1336	1216	1208	1144
pH	1.8	1.9	2.0	1.9	2.3	1.9	1.8	1.8

<sup>a</sup> Calculated by the difference, 100—(C + H + N).

Figure 6 compares the GC-MS chromatograms of the bio-oil products obtained at two temperatures of 440 and 480 °C, at a 0.8 kg/h sawdust feeding rate. The GC-MS analysis detected more than 140 organic compounds in the bio-oil products. The compounds with a benzene ring were formed at relatively high concentrations. Those phenolic compounds were mostly formed by decomposition of the lignin constituent of the sawdust feed [38]. Significant amounts of 1,6-anhydro-D-glucose (levoglucosan) and furfural derivatives from the decomposition of cellulosic components were also detected at both temperatures. A negligible change in the pattern and peak height of the chromatograms was observed over the pyrolysis temperature range of 440–480 °C, at which the bio-oil yield showed a high variation.

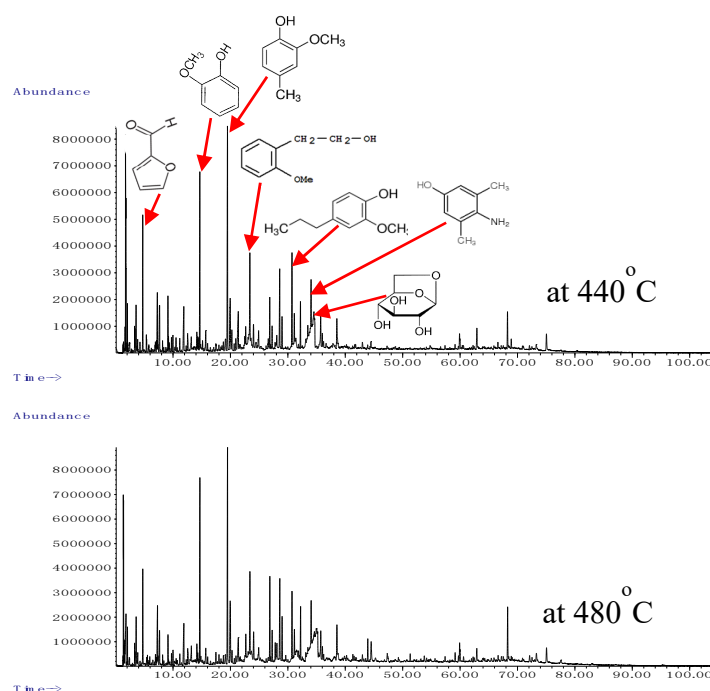
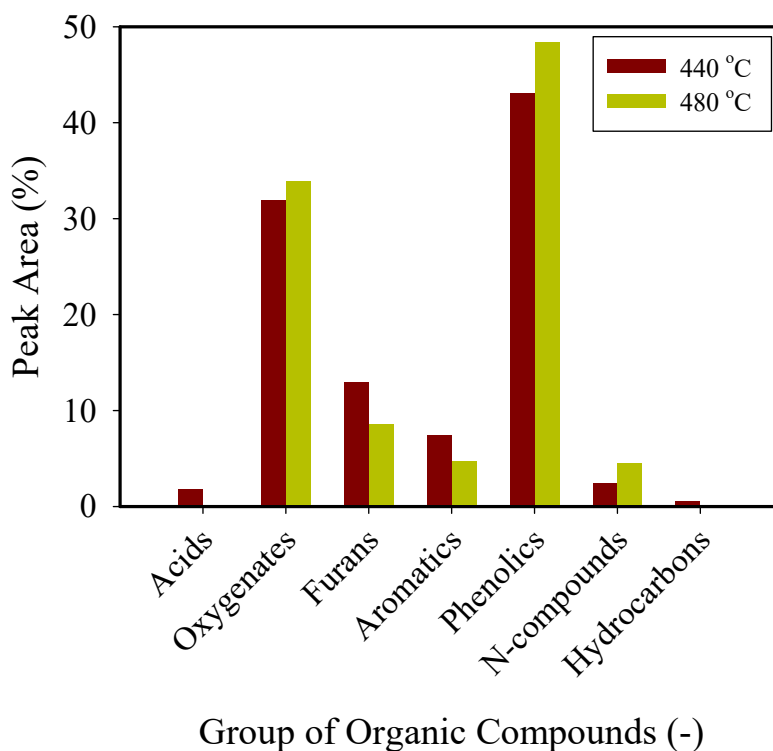
**Figure 6.** GC-MS chromatograms for bio-oil (0.8 kg/h feeding rate, 15 L/min N<sub>2</sub> carrier gas flow rate).

Table 3 lists 32 major compounds detected in the bio-oil products at different pyrolysis temperatures of 440 and 480 °C. Phenolic compounds such as 2-methoxy phenol, 2-methoxy (guaiacol), 2-methoxy-4-methyl phenol (cresol), and 2-methoxy-4(1-propenyl) phenol were the most prevalent compounds among the benzene ring-containing products and remained at high levels in the bio-oil with increased pyrolysis temperature from 440 °C to 480 °C. The higher temperature also favored

the formation of levoglucosan. This is an unexpected result because levoglucosan is known to be a compound which is first formed during the decomposition of cellulose, and then undergoes further degradation reactions to form furan derivatives and acids. Probably, pyrolysis temperatures below 480 °C are too low to achieve complete decomposition of cellulose to its unit compound, levoglucosan. Meanwhile higher pyrolysis temperatures promote the decomposition of furfurals and acids which might be produced from levoglucosan. The compounds present in the bio-oil products at the two pyrolysis temperatures were all grouped on the basis of their functionalities, as shown in Figure 7. Phenol derivatives from the decomposition of lignin fraction were more than 40 area % at 440 °C and increased to 48.3 area % at 480 °C, indicating that the phenol derivatives were relatively stable under the pyrolysis conditions. In a related work, Klemetsrud et al. [39] also found that a higher temperature favored the formation of phenolic species from the pyrolysis of hybrid poplar biomass. In the pyrolysis of Douglas-fir lignin, Zhou et al. [40] found a significant amount of guaiacol derivatives without the formation of monophenols. On the basis of their findings, they proposed lignin thermochemical conversion mechanisms consisting of two major steps in which the formation of lignin oligomers occurred relatively fast, and then the formed oligomer were further degraded to monophenols at lower reaction rates. The formation of nitrogen-containing compounds was consistent with the elemental analysis results and slightly increased with an increase in the pyrolysis temperature. Furan derivatives and acids were present in the bio-oil products at low levels, indicating that those compounds were not stable under the pyrolysis conditions.

**Table 3.** Comparison of major organic compounds in bio-oil products obtained at two different temperatures.

No.	RT (min)	Compound	Area (%)	
			440 °C	480 °C
1	4.722	Furfural	2.48	2.20
2	7.269	2(5H)-Furanone	1.77	2.24
3	7.658	1,2-Cyclopentanedione	1.99	1.44
4	9.111	Furfural, 5-methyl-	1.09	0.71
5	11.875	2-Cyclopenten-1-one, 2-hydroxy-3-methyl-	1.82	1.92
6	12.533	4-Methyl-5H-furan-2-one	0.73	0.87
7	14.147	Phenol, 4-methyl-	0.75	0.73
8	14.662	Phenol, 2-methoxy- (guaiacol)	4.62	5.45
9	15.692	Maltol	0.98	0.77
10	19.176	4H-Pyran-4-one, 3,5-dihydroxy-2-methyl-	0.88	0.58
11	19.480	Phenol, 2-methoxy-4-methyl- (cresol)	6.90	7.41
12	19.954	1,2-Benzenediol	2.92	3.86
13	20.241	1,4:3,6-Dianhydro-.alpha.-d-glucopyranose	0.73	0.48
14	21.368	2-Furancarboxaldehyde, 5-(hydroxymethyl)-	2.44	1.80
15	22.655	1,2-Benzenediol, 3-methyl-	0.67	1.06
16	23.382	Benzeneethanol, 2-methoxy-	3.05	3.31
17	24.017	4 Methyl catechol	0.95	1.53
18	24.904	2-Methoxy-4-vinylphenol	0.57	0.55
19	26.844	Phenol, 2-methoxy-3-(2-propenyl)-	1.36	2.54
20	27.262	Phenol, 2-methoxy-4-propyl-	0.57	0.94
21	28.578	Vanillin	2.46	3.32
22	30.723	Phenol, 2-methoxy-4-(1-propenyl)- (isoeugenol)	2.94	2.17
23	31.130	Phenol, 2-methoxy-4-propyl-	1.24	1.27
24	32.194	Ethanone, 1-(4-hydroxy-3-methoxyphenyl)-	1.24	1.70
26	33.476	Benzoic acid, 4-hydroxy-3-methoxy-, methyl ester	3.44	1.41
27	34.042	2,6-dimethyl-4-hydroxyaniline	1.38	4.13
28	34.311	d-Allose	3.55	1.61
29	34.546	1,6-Anhydro-.beta.-D-glucopyranose (levoglucosan)	2.96	6.50
30	36.005	propano 3-methoxy-4-hydroxyphenone	0.52	0.65
31	38.534	Benzeneacetic acid, 4-hydroxy-3-methoxy-	1.56	1.72
32	62.927	1-Phenanthrenecarboxylic acid	0.98	0.53
total			67.90	65.40



**Figure 7.** Distribution of organic compounds formed in bio-oil (0.8 kg/h feeding rate, 15 L/min N<sub>2</sub> carrier gas flow rate).

Table 4 summarizes fuel characteristics of the biochar product obtained at the reactor bottom char collector under the different temperatures and feeding rates. The proximate analysis results show a significant increase in fixed carbon content of the biochar products as compared with the sawdust feed. A significant amount of the volatile matter might be converted into organic compounds in the bio-oil products or gaseous products, while the crystalline cellulose carbon and lignin carbon remained in the biochar products. Ash content of the biochars was higher than the sawdust feed, due to the presence of a fraction of sand medium which over-flowed through the annulus. Nevertheless, the heating value of the biochar was over 24 kJ/kg accompanied with low O/C ratios in all the experiments. Azargohar et al. [41] found that the O/C ratio of biochar decreased with an increase in pyrolysis temperature due to the development of compact aromatic structure in the biochar byproduct.

**Table 4.** Effect of pyrolysis temperature and feeding rate on the fuel characteristics of the reactor bottom biochar.

	Pyrolysis Temperature (°C) at 0.84 kg/h Feeding Rate					Sawdust Feeding Rate (kg/h) at 440 °C		
	426	444	457	480	528	0.84	1.32	1.77
Yield (wt%)	28.7	22.7	21.6	21.5	20.10	22.7	24.4	25.54
Proximate anal. (wt%)								
Moisture content	3.5	3.2	3.3	3.4	3.3	3.2	2.9	3.1
Volatile matter	37.5	33.1	32.1	26.4	22.0	33.1	36.3	36.1
Fixed carbon	50.1	53.6	59.3	56.6	58.3	53.6	53.6	57.1
Ash	9.0	10.2	5.3	13.6	16.4	10.2	7.3	3.6
Elemental comp. (wt%)								
C	68.6	74.0	66.5	75.7	58.0	74.0	64.2	72.8
H	4.6	4.8	3.8	4.0	2.3	4.8	4.0	4.5
N	0.4	0.3	0.3	0.4	0.6	0.3	0.4	0.4
O <sup>a</sup>	26.4	20.9	29.4	19.9	39.1	20.9	31.4	22.3
O/C (mol/mol)	0.38	0.21	0.33	0.20	0.51	0.21	0.37	0.23
H/C (mol/mol)	0.80	0.78	0.69	0.63	0.48	0.78	0.75	0.74
HHV (MJ/kg)	25.33	26.62	26.08	26.71	24.32	26.62	24.40	25.87

<sup>a</sup> Calculated by the difference of 100—(C + H + N).

Table 5 compares physical and chemical properties of the biochar products obtained at the different places, reactor bottom char collector and cyclone, with operating conditions of 461 °C and 1.6 kg/h sawdust feeding rate. As expected, the reactor bottom biochar contained a little higher concentration of ash and fixed carbon due to the presence of sand media and crystalline cellulose carbon, respectively. Meanwhile, the cyclone carbon was found in a powder form and contained a relatively high amount of volatile matter, indicating the possibility that this cyclone char was formed by coking reactions of the pyrolysis vapors. The cyclone char has lower heating values than the reactor bottom char due to the higher content of oxygen.

**Table 5.** Comparison of biochar product obtained from the reactor bottom collector and the cyclone at 461 °C, 1.6 kg/h feeding rate, and 15 L/min N<sub>2</sub> carrier gas flow rate.

Biochar Product	Proximate Analysis (wt%)				Ultimate Analysis <sup>b</sup> (wt%)					Heating Value <sup>c</sup> (MJ/kg)	
	M <sup>a</sup>	VM	FC	Ash	C	H	N	S	O <sup>d</sup>	HHV	LHV
Reactor bottom	2.9	36.0	58.2	2.9	74.7	4.6	0.4	ND <sup>e</sup>	20.3	26.6	25.5
Cyclone	8.9	42.3	47.1	1.7	68.8	4.3	0.5	10 <sup>-3</sup>	26.4	24.9	23.7

<sup>a</sup> M, moisture; VM, volatile matter; FC, fixed carbon. <sup>b</sup> Ultimate analysis was on a dry basis. <sup>c</sup> Heating value was on a dry basis. <sup>d</sup> Calculated by the difference of 100—(C + H + N + S); <sup>e</sup> not detected.

The fast pyrolysis of the sawdust also produced significant amounts of the gaseous products with the yields of 12–39 wt% depending on the reaction condition. Major species detected included CO, CO<sub>2</sub>, and CH<sub>4</sub>. Negligible amounts of H<sub>2</sub>, C<sub>2</sub>-, and C<sub>3</sub>- hydrocarbons were also formed in all the experiments. Figure 8 shows the variation in the composition of the major gaseous products with pyrolysis temperature. The content of N<sub>2</sub> carrier gas decreased with increasing temperature to reach 41 vol% at 528 °C. The influence of pyrolysis temperature on the concentration of the gas constituents was not significant except for the case of CH<sub>4</sub> whose content was less than 0.1 vol% at 426 °C, but increased to 21.4 vol% at about 460 °C. It can be said that a pyrolysis temperature between 420 and 460 °C is one of the most important parameters to affect distribution and characteristics of the products from the fast pyrolysis of the sawdust feed in the double-tube type of BFB reactor.

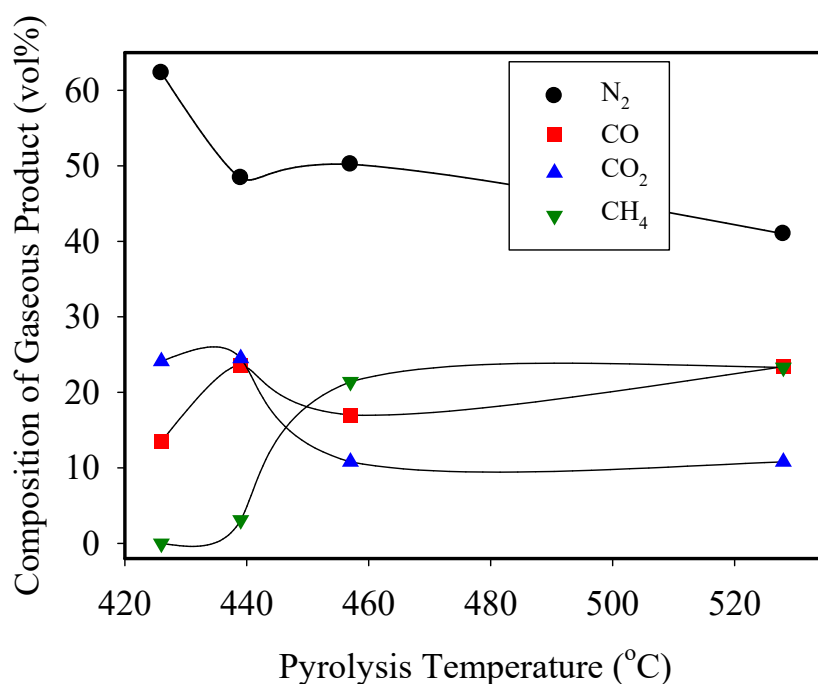


**Figure 8.** Variation in composition of gaseous product with pyrolysis temperature (0.8 kg/h feeding rate, 15 L/min N<sub>2</sub> carrier gas flow rate).

#### 4. Conclusions

Biomass fast pyrolysis usually produces bio-oil, biochar, and syngas. One of technical issues addressed in a bubbling fluidized bed (BFB) reactor for biomass fast pyrolysis is to maintain the bubbling bed at a constant level by removing biochar product from the bed in a steady mode. As a means to achieve this purpose, a double-tube type of BFB reactor was constructed and examined in the fast pyrolysis of pine wood sawdust. In this reactor, the bed level was mechanically controlled by the height of the inner tube in which biomass fast pyrolysis occurred. The significant amounts of biochar that formed in the inner tube were removed through the annulus between the inner and outer tubes of the reactor, thereby, the load of cyclone after the reactor was markedly reduced. The effect of pyrolysis temperature and wood sawdust feeding rate on the yields and characteristics of the products was examined under the conditions of 15 L/min nitrogen carrier gas flow rate and 0.5–1.0 mm particle sizes of the sawdust feed. A maximum bio-oil yield of 62.4 wt% was obtained at 440 °C. The sawdust feeding rate produced negligible influences on the product distribution. More than 79 wt% of the biochar product was removed from the bed, through the annulus into the reactor bottom collector. The bio-oil products showed higher heating values (HHVs) of 16.8–17.5 MJ/kg while the biochars showed HHVs of 24.4–26.7 MJ/kg, depending on the reaction conditions. The bio-oil products had water contents of 30.7–49.2 wt% along with low pH values between 1.8 and 2.3. The GC-MS analysis of the bio-oils found more than 140 organic compounds at pyrolysis temperatures of 440 and 480 °C. The detected compounds included reduced sugars, acids, furans, alcohols, ketones, phenols, and nitrogenous compounds.

**Author Contributions:** Conceptualization, I.-G.L.; methodology, I.-G.L.; investigation, I.-G.L., J.H.H.; data curation, I.-G.L., J.H.H.; writing—review and editing, I.-G.L.; supervision, I.-G.L.; project administration, I.-G.L.; funding acquisition, I.-G.L. All authors have read and agreed to the published version of the manuscript.

**Funding:** This research was funded by the New & Renewable Energy Core Technology Program of the Korea Institute of Energy Technology Evaluation and Planning (KETEP), granted financial resource from the Ministry of Trade, Industry & Energy, Republic of Korea (no. 20143030090940) and the National Research Council of Science & Technology (NST) grant by the Korea Government (MSIP), Republic of Korea (no. CAP-16-05-KIMM).

**Conflicts of Interest:** The authors declare no conflict of interest.

#### References

1. Bauen, A.; Berndes, G.; Junginger, M.; Londo, M.; Vuille, F. Bioenergy—A sustainable and reliable energy source, A review of status and prospects. *IEA Bioenergy Annu. Rep.* **2009**, *5*, 108.
2. Saidur, R.; Abdelaziz, E.A.; Demirbas, A.; Hossain, M.S.; Mekhilef, S. A review on biomass as a fuel for boilers. *Renew. Sustain. Energy Rev.* **2011**, *15*, 2262–2289. [[CrossRef](#)]
3. Tillman, D.A. Biomass cofiring: The technology, the experience, the combustion consequences. *Biomass Bioenergy* **2000**, *19*, 365–384. [[CrossRef](#)]
4. Míguez, J.L.; Morán, J.C.; Granada, E.; Porteiro, J. Review of technology in small-scale biomass combustion systems in the European market. *Renew. Sustain. Energy Rev.* **2012**, *16*, 3867–3875. [[CrossRef](#)]
5. Panwar, N.L.; Kothari, R.; Tyagi, V.V. Thermo chemical conversion of biomass—Eco friendly energy routes. *Renew. Sustain. Energy Rev.* **2012**, *16*, 1801–1816. [[CrossRef](#)]
6. Bridgwater, A.V.; Peacocke, G.V.C. Fast pyrolysis processes for biomass. *Renew. Sustain. Energy Rev.* **2000**, *4*, 1–73. [[CrossRef](#)]
7. Huang, H.; Yuan, X. Review: Recent progress in the direct liquefaction of typical biomass. *Prog. Energy Combust. Sci.* **2015**, *49*, 59–80. [[CrossRef](#)]
8. Ahmad, A.A.; Zawawi, N.A.; Kasim, F.H.; Inayat, A.; Khasri, A. Assessing the gasification performance of biomass: A review on biomass gasification process conditions, optimization and economic evaluation. *Renew. Sustain. Energy Rev.* **2016**, *53*, 1333–1347. [[CrossRef](#)]
9. Swain, P.K.; Das, L.M.; Naik, S.N. Biomass to liquid: A prospective challenge to research and development in 21st century. *Renew. Sustain. Energy Rev.* **2011**, *15*, 4917–4933. [[CrossRef](#)]

10. Trippe, F.; Fröhling, M.; Schultmann, F.; Stahl, R.; Henrich, E.; Dalai, A. Comprehensive techno-economic assessment of dimethyl ether (DME) synthesis and Fischer-Tropsch synthesis as alternative process steps within biomass-to-liquid production. *Fuel Process. Technol.* **2013**, *106*, 577–586. [[CrossRef](#)]
11. Elliott, D.C.; Biller, P.; Ross, A.B.; Schmidt, A.J.; Jones, S.B. Hydrothermal liquefaction of biomass: Developments from batch to continuous process. *Bioresour. Technol.* **2015**, *178*, 147–156. [[CrossRef](#)] [[PubMed](#)]
12. Kan, T.; Strezov, V.; Evans, T.J. Lignocellulosic biomass pyrolysis: A review of product properties and effects of pyrolysis parameters. *Renew. Sustain. Energy Rev.* **2016**, *57*, 1126–1140. [[CrossRef](#)]
13. Lu, Q.; Li, W.Z.; Zhu, X.F. Overview of fuel properties of biomass fast pyrolysis oils. *Energy Convers. Manag.* **2009**, *50*, 1376–1383. [[CrossRef](#)]
14. Lehto, J.; Oasmaa, A.; Solantausta, Y.; Kytö, M.; Chiaramonti, D. Review of fuel oil quality and combustion of fast pyrolysis bio-oils from lignocellulosic biomass. *Appl. Energy* **2014**, *116*, 178–190. [[CrossRef](#)]
15. Czernik, S.; Bridgwater, A.V. Overview of applications of biomass fast pyrolysis oil. *Energy Fuels* **2004**, *18*, 590–598. [[CrossRef](#)]
16. No, S.Y. Application of bio-oils from lignocellulosic biomass to transportation, heat and power generation—A review. *Renew. Sustain. Energy Rev.* **2014**, *40*, 1108–1125. [[CrossRef](#)]
17. Mercader, F.D.M.; Groeneveld, M.J.; Kersten, S.R.A.; Venderbosh, R.H.; Hogendoorn, J.A. Pyrolysis oil upgrading by high pressure thermal treatment. *Fuel* **2010**, *89*, 2829–2837. [[CrossRef](#)]
18. Patel, M.; Kumar, A. Production of renewable diesel through the hydroprocessing of lignocellulosic biomass-derived bio-oil: A review. *Renew. Sustain. Energy Rev.* **2016**, *58*, 1293–1307. [[CrossRef](#)]
19. Rezaei, P.S.; Shafaghat, H.; Daud, W.M.A.W. Production of green aromatics and olefins by catalytic cracking of oxygenate compounds derived from biomass pyrolysis: A review. *Appl. Catal. A Gen.* **2014**, *469*, 490–511. [[CrossRef](#)]
20. Bahng, M.K.; Mukarakate, C.; Robichaud, D.J.; Nimlos, M.R. Current technologies for analysis of biomass thermochemical processing: A review. *Anal. Chim. Acta* **2009**, *651*, 117–138. [[CrossRef](#)]
21. Ishak, W.N.R.W.; Hisham, M.W.M.; Yarmo, M.A.; Hin, T.Y. A review on bio-oil production from biomass by using pyrolysis method. *Renew. Sustain. Energy Rev.* **2012**, *16*, 5910–5923. [[CrossRef](#)]
22. Vardiambasis, I.O.; Kapetanakis, T.N.; Nikolopoulos, C.D.; Trang, T.K.; Tsubota, T.; Keyikoglu, R.; Khataee, A.; Kalderis, D. Hydrochars as emerging biofuels: Recent advances and application of artificial neural networks for the prediction of heating values. *Energies* **2020**, *13*, 4572. [[CrossRef](#)]
23. Venderboasch, R.H.; Prins, W. Fast pyrolysis technology development. *Biofuels Bioprod. Biorefin.* **2010**, *4*, 178–208. [[CrossRef](#)]
24. Solantausta, Y.; Oasmaa, A.; Sipilar, K.; Lindfors, C.; Lehto, J.; Autio, J.; Jokela, P.; Alin, J.; Heiskanen, J. Bio-oil production from biomass: Steps toward demonstration. *Energy Fuels* **2012**, *26*, 233–240. [[CrossRef](#)]
25. Karmee, S.K.; Kumari, G.; Soni, B. Pilot scale oxidative fast pyrolysis of sawdust in a fluidized bed reactor: A biorefinery approach. *Bioresour. Technol.* **2020**, *318*, 124071. [[CrossRef](#)]
26. Chen, B.; Han, X.; Tong, J.; Mu, M.; Jiang, X.; Wang, S.; Shen, J.; Ye, X. Studies of fast co-pyrolysis of oil shale and wood in a bubbling fluidized bed. *Energy Convers. Manag.* **2020**, *205*, 112356. [[CrossRef](#)]
27. Santamaria, L.; Beirrow, M.; Mangold, F.; Lopez, G.; Olazar, M.; Schmid, M.; Li, Z.; Scheffknecht, G. Influence of temperature on products from fluidized bed pyrolysis of wood and solid recovered fuel. *Fuel* **2021**, *283*, 118922. [[CrossRef](#)]
28. Xianwen, D.; Chuangzhi, W.; Haibin, L.; Yong, C. The fast pyrolysis of biomass in CFB reactor. *Energy Fuels* **2000**, *14*, 552–557. [[CrossRef](#)]
29. Park, J.Y.; Kim, J.K.; Oh, C.H.; Park, J.W.; Kwon, E.E. Production of bio-oil from fast pyrolysis of biomass using a pilot-scale circulating fluidized bed reactor and its characterization. *J. Environ. Manag.* **2019**, *234*, 138–144. [[CrossRef](#)]
30. Dupont, C.; Commandré, J.M.; Gauthier, P.; Boissonnet, G.; Salvador, S.; Schweich, D. Biomass pyrolysis experiments in an analytical entrained flow reactor between 1073 K and 1273 K. *Fuel* **2008**, *87*, 1155–1164. [[CrossRef](#)]
31. Ashcraft, R.W.; Heynderickx, G.J.; Marin, G.B. Modeling fast biomass pyrolysis in a gas-solid vortex reactor. *Chem. Eng. J.* **2012**, *207*, 195–208. [[CrossRef](#)]

32. Johansson, A.C.; Wiinikka, H.; Sandström, L.; Marklund, M.; Öhrman, O.G.W.; Narvesjö, J. Characterization of pyrolysis products produced from different Nordic biomass types in a cyclone pilot plant. *Fuel Process. Technol.* **2016**, *146*, 9–19. [[CrossRef](#)]
33. Trinh, T.N.; Jensen, P.A.; Sárossy, Z.; Dam-Johansen, K.; Knudsen, N.O.; Sørensen, H.R.; Egsgaard, H. Fast pyrolysis of lignin using a pyrolysis centrifuge reactor. *Energy Fuels* **2013**, *27*, 3802–3810. [[CrossRef](#)]
34. Gable, P.; Brown, R.C. Effect of biomass heating time on bio-oil yields in a free fall fast pyrolysis reactor. *Fuel* **2016**, *166*, 361–366. [[CrossRef](#)]
35. Li, J. The optimal of pyrolysis process in the rotating cone reactor and pyrolysis product analysis. In Proceedings of the International Conference on Challenges in Environmental Science and Computer Engineering, SESCE 2010, Wuhan, China, 6–7 March 2010; Volume 1, pp. 530–533.
36. Luz, F.C.; Cordiner, S.; Manni, A.; Mulone, V.; Rocco, V. Biomass fast pyrolysis in screw reactors: Prediction of spent coffee grounds bio-oil production through a monodimensional model. *Energy Convers. Manag.* **2018**, *168*, 98–106.
37. Park, H.J.; Park, Y.K.; Kim, J.S. Influence of reaction conditions and the char separation system on the production of bio-oil from radiate pine sawdust by fast pyrolysis. *Fuel Process. Technol.* **2008**, *89*, 797–802.
38. Muley, P.D.; Henkel, C.; Abdollahi, K.K.; Marculescu, C.; Boldor, D. A critical comparison of pyrolysis of cellulose, lignin, and pine sawdust using an induction heating reactor. *Energy Convers. Manag.* **2016**, *117*, 273–280. [[CrossRef](#)]
39. Klemetsrud, B.; Eatherton, D.; Shonnard, D. Effects of lignin content and temperature on the properties of hybrid poplar bio-oil, char, and gas obtained by fast pyrolysis. *Energy Fuels* **2017**, *31*, 2879–2886. [[CrossRef](#)]
40. Zhou, S.; Pecha, B.; Kuppevelt, M.V.; McDonald, A.G.; Garcia-Perez, M. Slow and fast pyrolysis of Douglas-fir lignin: Importance of liquid-intermediate formation on the distribution of products. *Biomass Bioenergy* **2014**, *6*, 398–409. [[CrossRef](#)]
41. Azargohar, R.; Nanda, S.; Kozinski, J.A.; Dalai, A.K.; Sutarto, R. Effects of temperature on the physicochemical characteristics of fast pyrolysis bio-chars derived from Canadian waste biomass. *Fuel* **2014**, *125*, 90–100. [[CrossRef](#)]

**Publisher’s Note:** MDPI stays neutral with regard to jurisdictional claims in published maps and institutional affiliations.



© 2020 by the authors. Licensee MDPI, Basel, Switzerland. This article is an open access article distributed under the terms and conditions of the Creative Commons Attribution (CC BY) license (<http://creativecommons.org/licenses/by/4.0/>).